haematologica
Journal of the Ferrata Storti Foundation

Acute myeloid leukemia drug tolerant persister cells survive chemotherapy by transiently increasing plasma membrane rigidity, that also increases their sensitivity to immune cell killing

by Yael Morgenstern, JongBok Lee, Yoosu Na, Brandon Y. Lieng, Nicholas S. Ly, William D. Gwynne, Rose Hurren, Li Ma, Dakai Ling, Marcela Gronda, Andrea Arruda, Avraham Frisch, Tsila Zuckerman, Yishai Ofran, Mark D. Minden, Li Zhang, Catherine O'Brien, Andrew T. Quaile, J. Rafael Montenegro-Burke, and Aaron D. Schimmer

Received: June 5, 2024.
Accepted: November 14, 2024.

Citation: Yael Morgenstern, JongBok Lee, Yoosu Na, Brandon Y. Lieng, Nicholas S. Ly, William D. Gwynne, Rose Hurren, Li Ma, Dakai Ling, Marcela Gronda, Andrea Arruda, Avraham Frisch, Tsila Zuckerman, Yishai Ofran, Mark D. Minden, Li Zhang, Catherine O'Brien, Andrew T. Quaile, J. Rafael Montenegro-Burke, and Aaron D. Schimmer. Acute myeloid leukemia drug tolerant persister cells survive chemotherapy by transiently increasing plasma membrane rigidity, that also increases their sensitivity to immune cell killing.
Haematologica. 2024 Nov 21. doi: 10.3324/haematol.2024.286018 [Epub ahead of print]

Acute myeloid leukemia drug tolerant persister cells survive chemotherapy by transiently increasing plasma membrane rigidity, that also increases their sensitivity to immune cell killing

Yael Morgenstern[1], JongBok Lee[2], Yoosu Na[2], Brandon Y. Lieng[3], Nicholas S. Ly[3], William D. Gwynne[3], Rose Hurren[1], Li Ma[1], Dakai Ling[1], Marcela Gronda[1], Andrea Arruda[1], Avraham Frisch[4], Tsila Zuckerman[4], Yishai Ofran[5], Mark D. Minden[1], Li Zhang[2], Catherine O'Brien[1], Andrew T. Quaile[3], J. Rafael Montenegro-Burke[3], Aaron D. Schimmer*[1]

1 Princess Margaret Cancer Centre, University Health Network, Toronto, Canada

2 Toronto General Hospital Research Institute, University Health Network, Toronto, Canada

3 Terrence Donnelly Centre for Cellular and Biomolecular Research, University of Toronto, Toronto, Canada

4 Department of Hematology and Bone Marrow Transplantation, Rambam Health Care Campus, Haifa, Israel

5 Hematology and Stem cell transplantation department and the Eisenberg R&D Authority, Shaare Zedek medical center, Hebrew University Jerusalem, Israel

* Contact:
Aaron D. Schimmer, MD, PhD, FRCPC
Princess Margaret Cancer Centre, University Health Network
Room 8-706; 101 College St.
Toronto, ON
M5G 1L7
Canada
Tel: 416-946-2838
Aaron.schimmer@uhn.ca

Contributions

Y.M designed and performed the experiments, analyzed data and wrote the article. J.B.L, Y.N, B.Y.L., N.S.L, W.D.G, R.H. L.M, D.L, M.G, A.T.Q, and J.R.M-B performed the experiments and analyzed data. A.A, A.F, T.Z, Y.O, M.D.M provided AML patient samples for the study. L.Z and C.O provided feedback and edited the manuscript. A.D.S conceived and designed the study.

Funding

This work was supported by the Canadian Institutes of Health Research the Leukemia and Lymphoma Society of Canada and the Princess Margaret Cancer Centre Foundation. ADS holds the Ronald N. Buick Chair in Oncology Research.

Data-sharing statement

Data files will be made available upon reasonable request to the corresponding authors.

Acknowledgments

We thank Jill Flewelling (Princess Margaret Cancer Centre) for administrative assistance.

Competing Interest Statement

A.D.S. has received research funding from Takeda Pharmaceuticals, BMS and Medivir AB, and consulting fees/honorarium from Takeda, Astra-Zeneca, BMS, and Novartis, Pharmaceuticals. A.D.S. is on the medical and scientific board of the Leukemia and Lymphoma Society of Canada. L.Z. has financial interests (e.g., holdings/shares) in WYZE Biotech Co Ltd and previously received research funding and consulting fee/honorarium from the company. A.D.S, L.Z. and J.L. are co-inventors of several DNT cell technology related patents and intellectual properties for the treatment of AML.

Abstract

Resistance to chemotherapy remains a major hurdle to the cure of Acute Myeloid Leukemia (AML) patients. Recent studies indicate a minority of malignant cells, termed drug-tolerant persisters (DTPs), stochastically upregulate stress pathways to evade cell death upon acute exposure to chemotherapy without acquiring new genetic mutations. This chemoresistant state is transient and the cells return to baseline after removal of chemotherapy. Yet, the mechanisms employed by DTPs to resist chemotherapy are not well understood and it is largely unknown whether these mechanisms are also seen in patients receiving chemotherapy. Here, we used leukemia cell lines, primary AML patient samples and samples from patients with AML receiving systemic chemotherapy to study the DTP state. We demonstrated that a subset of AML cells transiently increases membrane rigidity to resist killing due to acute exposure to Daunorubicin and Ara-C. Upon removal of the chemotherapy, membrane rigidity returned to baseline and the cells regained chemosensitivity. Although resistant to chemotherapy, the increased membrane rigidity, rendered AML cells more susceptible to T-cell mediated killing. Thus, we identified a novel mechanism by which DTP leukemic cells evade chemotherapy and a strategy to eradicate these persistent cells.

Introduction

Acute Myeloid Leukemia (AML) is a clonal disorder affecting early hematopoietic cells. It is an aggressive hematologic malignancy with a generally unfavorable prognosis. While several new therapeutic approaches for AML have been approved in recent years, conventional treatment still involves induction chemotherapy with a combination of chemotherapeutic agents, Ara-C and Daunorubicin. Despite high initial response rates to induction chemotherapy, failure to achieve remission after one or two cycles of treatment is not unusual and continues to present a therapeutic challenge. Patients whose disease is refractory to first-line induction therapy have a dismal prognosis with a 5-year survival of only 17%[1]. Predictors of non-response to Ara-C and Daunorubicin induction chemotherapy include poor risk cytogenetics, high risk molecular aberrations such as p53 mutations[2], a cell hierarchy composition enriched for primitive, non-mature leukemic cells[3] and residual leukemic cells in the marrow at early times after chemotherapy (ie: days 5-14 post chemotherapy)[4,5].

Classically, resistance to treatment in AML is attributed to leukemic stem cells (LSC). These cells are present at diagnosis and are inherently resistant to chemotherapy[6–8]. However, recent studies in AML, and other malignancies, report an additional mechanism of resistance, mediated by a non-LSCs drug-tolerant persister (DTP) cell population. DTPs alter their cellular state following treatment[9], leading to the development of an acute and transient resistance to chemotherapy[10–13]. When the stress of chemotherapy is removed, the cellular state returns to baseline and the cells regain sensitivity to chemotherapy.

DTPs have been reported in several types of cancer including breast[14,15], colorectal[16], and lung[17,18] where they confer chemoresistance and contribute to disease relapse. DTP cells transiently upregulate stress mitigation pathways to facilitate their survival during therapy, without the acquisition of new genetic mutations. For example, enrichment in a diapause gene signature was detected in colon cancer and breast cancer DTP cells, reminiscent of an evolutionary conserved embryonic strategy employed to survive unfavorable conditions[14,16]. DTP cells arise stochastically[19] during treatment and express a unique phenotype consisting of a slow proliferation rate[20] and a metabolic shift to increased autophagy[20] and fatty acid oxidation[11,19,21,22]. Notably,

persistent cells that succeed in avoiding the effect of anti-cancer treatment, regain drug sensitivity upon drug removal, underscoring the plasticity of DTP cells and suggesting a timed window of opportunities for targeting this population. However, whether chemotherapy-resistant DTP cells are relevant in AML is unknown.

Here, we identified DTP cells in AML with alterations in their lipid and elongation of fatty acids. This shift manifested as changes in the physical characteristics of the cell membrane, enhancing membrane rigidity. Notably, cell membrane rigidity boosted the susceptibility of DTP cells to T-cell-mediated killing. Our findings indicate a novel mechanism for chemoresistance in the DTP state and highlight T-cell-based immunotherapeutic approaches as a strategy to eliminate these resistant cells.

Methods

Primary AML and normal hematopoietic cells

Primary human AML samples were obtained from peripheral blood or bone marrow of both male and female patients with AML, following informed consent, and then cryopreserved. Approval for the collection and use of the primary samples was obtained from the UHN Research Ethics Board and the Rambam Health Care Campus. AML cells were isolated using Ficoll-Paque differential density centrifugation and subsequently frozen in a solution comprising 50% FCS, 40% αMEM, and 10% dimethylsulfoxide. Information about the patients who were the source of the cells is provided in supplemental Table 1.

Drug tolerant persister (DTP) model

MV4-11, MOLM13, THP-1, NB4, OCI-AML2 and OCI-AML3 cells were treated with Daunorubicin and Ara-C at IC90 concentrations for 5 days. Concentrations of drugs used for each cell line are: MV4-11- 20 nM Daunorubicin/ 70 nM Ara-C; MOLM13- 40 nM Daunorubicin/ 200 nM Ara-C; THP-1 - 90 nM Daunorubicin/ 900 nM Ara-C; NB4 – 30 nM Daunorubicin/ 150 nM Ara-C; OCI-AML2 – 60 nM Daunorubicin/ 600 nM Ara-C; OCI-AML3 - 90 nM Daunorubicin/ 900 nM Ara-C; Dead cells were removed on day 6

post-treatment via magnetic column depletion using the cell death removal kit (Miltenyi Biotec) according to the company's instructions.

Membrane fluidity

Membrane fluidity was assessed using pyrenedecanoic acid (PDA; Membrane Fluidity Kit; Abcam). Cells were incubated at room temperature with the labeling solution containing 5µM of fluorescent lipid reagent and 0.08% Pluronic F127, for 1 hour. Cells were washed and then plated in a 96-well plate at a final volume of 100uL. Fluorescence intensities were measured using a plate reader with excitation at 350 nm and emissions at 400 nm (monomer) and 470 nm (excimer) emissions. Patient samples membrane fluidity was measured by using flow cytometry, gating on the $CD45^{dim}CD34^{+}CD117^{+}$ population to obtain median fluorescence intensity (MFI) at 400 nm (monomer) and 470 nm (excimer) emissions. Membrane fluidity was assessed by calculating the ratio of 470 (excimer)/440 (monomer) fluorescence.

Membrane fluidity was also measured by staining cells with Di-4-ANEPPDHQ (Di4) (ThermoFisher, D36802) as previously described[23]. Cells were incubated with 1 µM Di4 for 20 minutes in room temperature. Di4 was excited at 488 nm and the fluorescence emission intensity of Di4 was recorded across the FITC and PerCP channels, representing ordered and disordered wavelength respectively. The Generalized Polarization (GP) value, reflecting relative membrane rigidity, was calculated as previously described[23]:

$$GP = \frac{Intensity\ Ordered - Intensity\ Disordered}{Intensity\ Ordered + Intensity\ Disordered}$$

Please see the Online Supplementary Appendix for additional methods

Results

Leukemic drug-tolerant persisters transiently resist cell death from chemotherapy

Standard induction chemotherapy for patients with AML involves a combination of Daunorubicin and Ara-C. To investigate drug-tolerant persisters (DTP) that survive the

acute exposure to chemotherapy, we treated MOLM13, MV4-11, and THP-1 leukemia cells with a combination of Daunorubicin and Ara-C at an IC_{90} for 5 days to mimic standard therapy. Viable cells that persisted after chemotherapy were collected 6 days post-treatment and replated into fresh media. The DTP cells exhibited a lag phase in proliferation for days 6-14 after chemotherapy (Figure 1A, *Online Supplementary Figure S1A*), but subsequently regained normal proliferation (Figure 1B, *Online Supplementary Figure S1B*). We then retreated the recovered leukemic cells with chemotherapy and these cells retained sensitivity equivalent to the wild-type leukemic cells (Figure 1C, *Online Supplementary Figure S1C*), underscoring the plasticity of these cells and the DTP state.

Quiescence and cell cycle delay are characteristic of the DTP state. Therefore, we measured cell cycle and EdU uptake in our DTP leukemic cells. We observed cell cycle delay in the DTP leukemic cells as evidenced by a decrease in the percentage of cells in the S-phase compared to parental cells and accumulation at the G1 or G2-M phase (Figure 1D, *Online Supplementary Figure S1D*). Of note, THP-1 DTP cells arrested at the G1 phase while the other cell lines arrested at the G2-M phase.

Although delayed in cell cycle, the DTP cells continued to proliferate albeit slower than the wild type cells (Figure 1E, *Online Supplementary Figure S1E*). In addition, we measured dilution of CellTrace Violet as an additional marker of proliferation. The population of DTP cells demonstrated decreased CellTrace Violet staining on day 5 compared to day 1, although the reduction was less pronounced than in the control cells (Figure 1F), indicating slow proliferation of the DTP cells. Thus, our model recapitulates key features of the DTP state.

Finally, we compared the intracellular levels of Daunorubicin in DTP and control cells. DTP and control cells were treated with increasing concentrations of Daunorubicin for 3 hours. After incubation, intracellular levels of Daunorubicin were measured by flow cytometry. Compared to control cells, DTP cells accumulated less Daunorubucin intracellularly (*Online Supplementary Figure S1F*).

Leukemic DTP cells alter lipidome composition

To understand mechanisms by which DTP leukemic cells resist chemotherapy, we conducted an unbiased analysis of the cellular lipidome 6 days post-chemotherapy. The lipidome heterogeneity in the different leukemic cells resulted in cell line specific lipidome rearrangement. However, we focused our analysis on lipidomic changes common to the three tested cell lines.

Compared to control cells, MOLM13, MV4-11 and THP-1 DTP cells that resisted the acute exposure to chemotherapy had increased elongated phosphatidylcholine (PC) with fatty acids chain lengths of more than 35 carbon atoms (Figure 2A, Online Supplementary Figure S2A), elongated triglycerides (TG) with a chain length of more than 53 carbon atoms (Figure 2B, *Online Supplementary Figure S2B*) and elongated phosphatidylethanolamine (PE) (Figure 2C). Additionally, an increase in the abundance of sphingomyelins (SM) of different fatty acid lengths were detected in the DTP cells (Figure 2D). In contrast, levels of cholesterol in the DTP cells were unchanged compared to the untreated cells (*Online Supplementary Figure S2C*).

To understand potential mechanisms for the increased elongated fatty acids, we measured fatty acid uptake in control and DTP leukemia cells. Compared to untreated controls, DTP leukemia cells increased uptake of fatty acids from the media, despite being in a slow cycle state (Figure 2E, *Online Supplementary Figure S2D*).

Leukemic DTP cells have increased membrane rigidity

Alterations in fatty acids influence the biophysical properties and fluidity of the cell membrane[24]. Specifically, elongation of fatty acids in membrane lipids and increased abundance of sphingomyelins increases membrane rigidity[25–27]. Previously, we and others demonstrated that increased plasma membrane rigidity decreases the intracellular accumulation of chemotherapy and renders cells chemo-resistant[28–31]. Therefore, given the increased elongated fatty acids and sphingomyelins in DTP leukemia cells, we measured membrane fluidity by staining DTP and control cells with the fluorescent dye, lipophilic pyrenedecanoic acid (PDA). PDA is a fluorescent probe that integrates into the cell membrane, emitting two distinct spectra based on the

membrane's fluidity. In MOLM13, MV4-11, THP1, NB4, OCI-AML2 and OCI-AML3 cells, membrane fluidity decreased (ie: membrane rigidity increased) in the DTP population (Figure 3A). We confirmed increased membrane rigidity in the DTP cells by staining cells with di-4-ANEPPDHQ, a dye whose fluorescence reflects lipid-packing order in biomembranes[23] (*Online Supplementary Figure 3*). Importantly, when the DTP cells regained normal proliferation and chemosensitivity, their membrane fluidity returned to basal levels similar to control cells (Figure 3A).

To extend our investigation of membrane fluidity and the DTP state in vivo to primary AML cells, we engrafted primary AML cells into NSG mice. Eight weeks after cell injection, mice were treated with Ara-C (60 mg/kg/day) for 5 consecutive days and then sacrificed on day 8 (Figure 3B). Human $CD45^+$ $CD33^+$ leukemic cells in the mouse marrow were quantified by flow cytometry. Treatment with Ara-C decreased the leukemic burden in the mice over 3-fold compared to vehicle treated mice (Figure 3C). We isolated the residual leukemic cells flushed from the mouse marrow by magnetic separation and measured membrane fluidity in the leukemic cells. In alignment with our in-vitro DTP model, primary leukemic cells that persisted after Ara-C treatment had increased cell membrane rigidity (Figure 3D).

Next, we examined primary AML cells obtained from patients receiving systemic chemotherapy. Bone marrow samples were obtained before and on day 5 of induction chemotherapy with Daunorubucin and Ara-C and the leukemic cells were identified by flow cytometry analysis and gating on $CD45^{dim}$, $CD34^+$ $CD117^+$ cells, representing patients' blasts. Compared to pre-treatment, membrane fluidity in the AML cells was decreased (ie: rigidity increased) in the patient's leukemic cells that persisted on day 5 of chemotherapy (Figure 3E).

Non-pharmacologic models that transiently increase membrane rigidity confer chemoresistance

As a non-pharmacologic approach to examine the relationship between membrane rigidity and the DTP state, we incubated AML cells at 31°C. Temperature is a known factor influencing cell membrane fluidity[32–34], and indeed, we observed increased cell membrane rigidity after culturing AML cells at 31°C (Figure 4C). Reminiscent of the DTP

cell phenotype, cells cultured at 31°C remained viable and continued to proliferate, albeit slower (Figure 4A). Cells cultured at 31°C were resistant to chemotherapy compared to cells cultured at 37°C (Figure 4B). Importantly, the phenotypes of increased membrane rigidity, decreased proliferation, and chemoresistance, were all reversible upon returning the cells to 37°C (Figure 4A-C), in accord with the recovery phase observed in DTP cells after drug removal.

To further investigate the relationship between membrane rigidity and chemoresistance, we cultured MOLM13 cells with soluble cholesterol to increase the cholesterol of the cell membrane. Consistent with prior reports[35], supplementation with soluble cholesterol decreased membrane fluidity (Figure 4D). These cells were then treated with increasing concentrations of Daunorubicin for 3 hours, and Daunorubicin uptake was measured using flow cytometry. Cholesterol-treated AML cells with more rigid membranes showed decreased Daunorubicin uptake (Figure 4E), reinforcing the link between membrane rigidity and chemoresistance

DTP cells have increased sensitivity to T cell mediated killing.

Recently, in a murine model of melanoma, increasing cell membrane stiffness by cholesterol depletion sensitized melanoma cells to T-cell-mediated killing[36]. The observed increase in cell membrane rigidity in AML DTP cells prompted us to investigate the sensitivity of these cells to T-cell-mediated killing using Double negative T cells (DNT) as a model. CD3+ CD4- CD8-double negative T-cells (DNT cells) are a rare subpopulation of mature T cells found in healthy individuals and can be expanded ex-vivo over 1000-fold. DNT cells have anti-leukemic activity through perforin-dependent and independent mechanisms but are not toxic to normal hematopoietic cells[37–39]. Phase I clinical trials demonstrated the safety and potential efficacy of DNT cells in treating AML patients relapsed after allogeneic stem cell transplantation[40].To test how membrane rigidity influences sensitivity to T-cell mediated killing, we first used our 31^{o}C cell culture model. AML cell lines cultured at 31^{o}C displayed heightened sensitivity to DNT-cell-mediated killing compared to cells cultured at 37^{o}C (Figure 5A).

To further evaluate the sensitivity of DTP leukemic cells to killing by DNT cells, MOLM13 cells were injected into the femurs of NSG mice. Mice were treated with Ara-C daily for 5 days. After chemotherapy treatment, DNT cells were injected intravenously 4 and 6 days after completion of Ara-C, to target the chemoresistant persistent cells. Treatment of mice with Ara-C and DNT cells decreased the leukemic burden compared to treatment with either Ara-C or DNT cells alone (Figure 5B).

Next, we evaluated the sensitivity of persistent cells derived from primary AML patients to T cell-killing using DNT cells. Primary AML samples were engrafted into immune deficient mice and treated daily with Ara-C for 5 days. On day 8, the residual AML cells were collected and co-cultured ex-vivo with DNT cells. The persistent primary leukemic cells had increased susceptibility to T-cell mediated cytotoxicity compared to the AML cells isolated from mice not treated with chemotherapy (Figure 5C).

Finally, we tested sensitivity to T cell mediated killing in residual leukemia cells isolated from a patient receiving systemic induction chemotherapy with Daunorubicin and Ara-C. Bone marrow samples were collected prior to treatment and on day 5 of chemotherapy. Cells persisting on day 5 had increased membrane rigidity compared to pre-treatment cells (Figure 3E). Leukemic cells pre-treatment and on day 5 of treatment were enriched from the bone marrow sample by magnetic separation and co-cultured with DNT cells for 2 hours. Compared to pre-treatment, AML cells remaining on day 5 of chemotherapy, had increased sensitivity to T-cell mediated killing (Figure 5D). Thus, although AML cells transiently resist chemotherapy by increasing cell membrane rigidity, this increased membrane rigidity confered sensitivity to T-cell mediated killing, highlighting a strategy to eradicate these persisting cells.

Discussion

Despite advancements in treatment options, chemoresistance and refractory disease remain a leading cause of death in AML patients[41]. The presence of LSCs has long been implicated as a significant contributor to drug resistance. However, LSC-independent mechanisms of drug resistance also exist. Among those mechanisms, there is emerging interest in the transient DTP state. Yet, the mechanisms by which

leukemic DTP cells transiently resist chemotherapy and how to target these residual cells remains unclear. Here, we demonstrate that leukemic DTP have increased plasma membrane rigidity that contributes to chemoresistance but also increases sensitivity to immune-mediated killing.

To our knowledge, we are first to describe that AML DTP cells transiently increase plasma membrane rigidity to resist acute exposure to chemotherapy. To confirm that transient alterations in membrane rigidity influence chemosensitivity, we used cholesterol treatment and a non-pharmacologic model in which cells were cultured under colder temperatures to transiently increase membrane rigidity. We demonstrated that these cells were transiently resistant to chemotherapy. Our findings are consistent with prior studies that demonstrated increased membrane rigidity is associated with chemoresistance[29]. For example, increasing membrane rigidity in AML by applying biomechanical pressure decreases cellular uptake of daunorubicin and renders cells resistant to the drug[28]. Likewise, membrane rigidity was increased in lung and colorectal cells resistant to cisplatin and oxaliplatin, respectively[42–45]. While we demonstrated that DTP cells have increased plasma membrane rigidity, we concede that DTP cells also transiently upregulate other mechanisms that confer chemoresistance. As such, alterations in membrane rigidity are one mechanism of chemoresistance in these cells.

Leukemic DTP cells increased uptake of fatty acids and had increased levels of elongated fatty acids,triglycerides and sphingomyelins. Prior studies demonstrated that alterations in the length of fatty acids and triglycerides and the amount of sphingomyelins[27] influences membrane fluidity. For example, in rat insulinoma beta cells, exposure to elongated fatty acids elevates plasma membrane rigidity[46]. Triglycerides are localized to lipid droplets, acting as reservoirs of cellular fatty acids, which ultimately will be incorporated in the plasma membrane[47]. The abundance of triglycerides contributes to membrane rigidity in LPS-stimulated human neutrophils[48]. However, we also recognize that altering metabolism and fatty acid composition can affect metabolism and cellular processes beyond the plasma membrane and these changes may also influence sensitivity to chemotherapy.

Recent studies report that remodeling of cancer cells' cytoskeleton decreases membrane rigidity and reduces T-cell-mediated cytotoxicity[49]. Conversely, increasing cell stiffness through modifications in the cancer cell membrane or cytoskeleton enhances T-cell-mediated killing[36,50–52]. We demonstrated that leukemic DTP cells have increased sensitivity to T-cell mediating killing. For our model of T-cell mediated killing, we employed DNT cells. DNT cells are a rare population of T-cells that are cytotoxic to AML cells while sparing normal hematopoietic cells[37–39]. DNT cells can be collected from healthy donors, expanded ex-vivo and utilized as an "off-the-shelf" allogeneic T-cell therapy. Their efficacy was highlighted in a recent phase I clinical trial, where DNT treatment led to a 50% progression-free survival rate at 1 year in a subgroup of poor prognosis relapsed AML patients[40]. Thus, our findings suggest that cell membrane modifications during the DTP phase, presents an opportunity for selectively targeting the persistent cell population with a T-cell-based immunotherapy approach.

In conclusion, we delineate a transient non-genetic adaptation in AML DTP cells, marked by the acquisition of an abnormal cellular lipid profile, resulting in heightened membrane rigidity and subsequent treatment resistance. Although conferring resistance to chemotherapy, this transient alteration in the membrane also heightened the cells' susceptibility to T-cell-mediated elimination. Thus, these results suggest that T-cell-based immunotherapy could be used immediately following induction chemotherapy to eradicate surviving leukemic DTP cells that are important in mediating disease relapse.

References

1. Ferguson P, Hills RK, Grech A, et al. An operational definition of primary refractory acute myeloid leukemia allowing early identification of patients who may benefit from allogeneic stem cell transplantation. Haematologica. 2016;101(11):1351-1358.

2. Rücker FG, Schlenk RF, Bullinger L, et al. TP53 alterations in acute myeloid leukemia with complex karyotype correlate with specific copy number alterations, monosomal karyotype, and dismal outcome. Blood. 2012;119(9):2114-2121.

3. Zeng AGX, Bansal S, Jin L, et al. A cellular hierarchy framework for understanding heterogeneity and predicting drug response in acute myeloid leukemia. Nat Med. 2022;28(6):1212-1223.

4. Ofran Y, Hayun M, Leiba R, et al. Bone marrow blast elimination by the fifth day of 7 + 3 induction is the strongest predictor of potential cure in patients with acute myeloid leukemia younger than 61 years of age: A long-term follow-up of a multi-center prospective study. Am J Hematol. 2020;95(1):E3-E5.

5. Bertoli S, Bories P, Béné MC, et al. Prognostic impact of day 15 blast clearance in risk-adapted remission induction chemotherapy for younger patients with acute myeloid leukemia: long-term results of the multicenter prospective LAM-2001 trial by the GOELAMS study group. Haematologica. 2014;99(1):46-53.

6. Ding L, Ley TJ, Larson DE, et al. Clonal evolution in relapsed acute myeloid leukaemia revealed by whole-genome sequencing. Nature. 2012;481(7382):506-510.

7. Shlush LI, Mitchell A, Heisler L, et al. Tracing the origins of relapse in acute myeloid leukaemia to stem cells. Nature. 2017;547(7661):104-108.

8. Parkin B, Ouillette P, Li Y, et al. Clonal evolution and devolution after chemotherapy in adult acute myelogenous leukemia. Blood. 2013;121(2):369-377.

9. Li K, Du Y, Cai Y, et al. Single-cell analysis reveals the chemotherapy-induced cellular reprogramming and novel therapeutic targets in relapsed/refractory acute myeloid leukemia. Leukemia. 2023;37(2):308-325.

10. Duy C, Li M, Teater M, et al. Chemotherapy Induces Senescence-Like Resilient Cells Capable of Initiating AML Recurrence. Cancer Discov. 2021;11(6):1542-1561.

11. Farge T, Saland E, de Toni F, et al. Chemotherapy-resistant human acute myeloid leukemia cells are not enriched for leukemic stem cells but require oxidative metabolism. Cancer Discov. 2017;7(7):716-735.

12. Boyd AL, Aslostovar L, Reid J, et al. Identification of Chemotherapy-Induced Leukemic-Regenerating Cells Reveals a Transient Vulnerability of Human AML Recurrence. Cancer Cell. 2018;34(3):483-498.e5.

13. van Gastel N, Spinelli JB, Sharda A, et al. Induction of a Timed Metabolic Collapse to Overcome Cancer Chemoresistance. Cell Metab. 2020;32(3):391-403.e6.

14. Dhimolea E, de Matos Simoes R, Kansara D, et al. An Embryonic Diapause-like Adaptation with Suppressed Myc Activity Enables Tumor Treatment Persistence. Cancer Cell. 2021;39(2):240-256.e11.

15. Vinogradova M, Gehling VS, Gustafson A, et al. An inhibitor of KDM5 demethylases reduces survival of drug-tolerant cancer cells. Nat Chem Biol. 2016;12(7):531-538.

16. Rehman SK, Haynes J, Collignon E, et al. Colorectal Cancer Cells Enter a Diapause-like DTP State to Survive Chemotherapy. Cell. 2021;184(1):226-242.e21.

17. Ramirez M, Rajaram S, Steininger RJ, et al. Diverse drug-resistance mechanisms can emerge from drug-tolerant cancer persister cells. Nat Commun. 2016;7:10690.

18. Sharma SV, Lee DY, Li B, et al. A chromatin-mediated reversible drug-tolerant state in cancer cell subpopulations. Cell. 2010;141(1):69-80.

19. Oren Y, Tsabar M, Cuoco MS, et al. Cycling cancer persister cells arise from lineages with distinct programs. Nature. 2021;596(7873):576-582.

20. Li S, Song Y, Quach C, et al. Transcriptional regulation of autophagy-lysosomal function in BRAF-driven melanoma progression and chemoresistance. Nat Commun. 2019;10(1):1693.

21. Aloia A, Müllhaupt D, Chabbert CD, et al. A Fatty Acid Oxidation-dependent Metabolic Shift Regulates the Adaptation of BRAF-mutated Melanoma to MAPK Inhibitors. Clin Cancer Res. 2019;25(22):6852-6867.

22. Viale A, Pettazzoni P, Lyssiotis CA, et al. Oncogene ablation-resistant pancreatic cancer cells depend on mitochondrial function. Nature. 2014;514(7524):628-632.

23. Dinic J, Biverståhl H, Mäler L, Parmryd I. Laurdan and di-4-ANEPPDHQ do not respond to membrane-inserted peptides and are good probes for lipid packing. Biochim Biophys Acta. 2011;1808(1):298-306.

24. Harayama T, Riezman H. Understanding the diversity of membrane lipid composition. Nat Rev Mol Cell Biol. 2018;19(5):281-296.

25. Cevc G. How membrane chain-melting phase-transition temperature is affected by the lipid chain asymmetry and degree of unsaturation: an effective chain-length model. Biochemistry. 1991;30(29):7186-7193.

26. Pinto SN, Silva LC, Futerman AH, Prieto M. Effect of ceramide structure on membrane biophysical properties: the role of acyl chain length and unsaturation. Biochim Biophys Acta. 2011;1808(11):2753-2760.

27. Prenner E, Honsek G, Hönig D, Möbius D, Lohner K. Imaging of the domain organization in sphingomyelin and phosphatidylcholine monolayers. Chem Phys Lipids. 2007;145(2):106-118.

28. Nirmalanandhan VS, Hurren R, Cameron WD, et al. Increased pressure alters plasma membrane dynamics and renders acute myeloid leukemia cells resistant to daunorubicin. Haematologica. 2015;100(10):e406-e408.

29. Peetla C, Vijayaraghavalu S, Labhasetwar V. Biophysics of Cell Membrane Lipids in Cancer Drug Resistance: Implications for Drug Transport and Drug Delivery with Nanoparticles. Adv Drug Deliv Rev. 2013;65(13-14):1686-1698.

30. Ramu A, Glaubiger D, Magrath IT, Joshi A. Plasma membrane lipid structural order in doxorubicin-sensitive and -resistant P388 cells. Cancer Res. 1983;43(11):5533-5537.

31. Callaghan R, Stafford A, Epand RM. Increased accumulation of drugs in a multidrug resistant cell line by alteration of membrane biophysical properties. Biochim Biophys Acta. 1993;1175(3):277-282.

32. Shmeeda H, Kaspler P, Shleyer J, Honen R, Horowitz M, Barenholz Y. Heat acclimation in rats: modulation via lipid polyunsaturation. Am J Physiol Regul Integr Comp Physiol. 2002;283(2):R389-R399.

33. Kolomiytseva IK, Perepelkina NI, Zharikova AD, Popov VI. Membrane lipids and morphology of brain cortex synaptosomes isolated from hibernating Yakutian ground squirrel. Comp Biochem Physiol B Biochem Mol Biol. 2008;151(4):386-391.

34. Suri LNM, McCaig L, Picardi MV, et al. Adaptation to low body temperature influences pulmonary surfactant composition thereby increasing fluidity while maintaining appropriately ordered membrane structure and surface activity. Biochim Biophys Acta Biomembr. 2012;1818(7):1581-1589.

35. Bastiaanse EML, Atsma DE, Vandervalk LJM, Vanderlaarse A. Metabolic Inhibition of Cardiomyocytes Causes an Increase in Sarcolemmal Fluidity Which May Be Due to Loss of Cellular Cholesterol. Arch Biochem Biophys. 1995;319(2):350-354.

36. Lei K, Kurum A, Kaynak M, et al. Cancer-cell stiffening via cholesterol depletion enhances adoptive T-cell immunotherapy. Nat Biomed Eng 2021;5(12):1411-1425.

37. Merims S, Li X, Joe B, et al. Anti-leukemia effect of ex vivo expanded DNT cells from AML patients: a potential novel autologous T-cell adoptive immunotherapy. Leukemia. 2011;25(9):1415-1422.

38. Lee JB, Minden MD, Chen WC, et al. Allogeneic Human Double Negative T Cells as a Novel Immunotherapy for Acute Myeloid Leukemia and Its Underlying Mechanisms. Clin Cancer Res. 2018;24(2):370-382.

39. Chen B, Lee JB, Kang H, Minden MD, Zhang L. Targeting chemotherapy-resistant leukemia by combining DNT cellular therapy with conventional chemotherapy. J Exp Clin Cancer Res. 2018;37(1):88.

40. Tang B, Lee JB, Cheng S, et al. Allogeneic double-negative T cell therapy for relapsed acute myeloid leukemia patients post allogeneic hematopoietic stem cell transplantation: A first-in-human phase I study. Am J Hematol. 2022;97(7):E264-E267.

41. Shallis RM, Wang R, Davidoff A, Ma X, Zeidan AM. Epidemiology of acute myeloid leukemia: Recent progress and enduring challenges. Blood Rev. 2019;36:70-87.

42. Todor IN, Lukyanova NY, Chekhun VF. The lipid content of cisplatin- and doxorubicin-resistant MCF-7 human breast cancer cells. Exp Oncol. 2012;34(2):97-100.

43. Liang X, Huang Y. Physical state changes of membrane lipids in human lung adenocarcinoma A549 cells and their resistance to cisplatin. Int J Biochem Cell Biol. 2002;34(10):1248-1255.

44. Rebillard A, Tekpli X, Meurette O, et al. Cisplatin-Induced Apoptosis Involves Membrane Fluidification via Inhibition of NHE1 in Human Colon Cancer Cells. Cancer Res. 2007;67(16):7865-7874.

45. Shimolina L, Gulin A, Ignatova N, et al. The Role of Plasma Membrane Viscosity in the Response and Resistance of Cancer Cells to Oxaliplatin. Cancers (Basel). 2021;13(24):6165.

46. Wieder N, Fried JC, Kim C, et al. FALCON systematically interrogates free fatty acid biology and identifies a novel mediator of lipotoxicity. Cell Metab. 2023;35(5):887-905.e11.

47. Tirinato L, Pagliari F, Limongi T, et al. An Overview of Lipid Droplets in Cancer and Cancer Stem Cells. Stem Cells Int. 2017;2017:1656053.

48. May GL, Wright LC, Obbink KG, et al. Increased saturated triacylglycerol levels in plasma membranes of human neutrophils stimulated by lipopolysaccharide. J Lipid Res. 1997;38(8):1562-1570.

49. Liu Y, Zhang T, Zhang H, et al. Cell Softness Prevents Cytolytic T-cell Killing of Tumor-Repopulating Cells. Cancer Res. 2021;81(2):476-488.

50. Tello-Lafoz M, Srpan K, Sanchez EE, et al. Cytotoxic lymphocytes target characteristic biophysical vulnerabilities in cancer. Immunity. 2021;54(5):1037-1054.e7.

51. Basu R, Whitlock BM, Husson J, et al. Cytotoxic T Cells Use Mechanical Force to Potentiate Target Cell Killing. Cell. 2016;165(1):100-110.

52. Saitakis M, Dogniaux S, Goudot C, et al. Different TCR-induced T lymphocyte responses are potentiated by stiffness with variable sensitivity. Elife. 2017;6:23190.

Figure legends

Figure 1: An in-vitro model for AML DTP cells

MOLM13 drug tolerant persistent (DTP) cells were treated with the combination of Daunorubicin (40nM) and Ara-C (200nM respectively) to achieve an IC^{90}. Residual viable cells were collected on day 6 after Daunorubicin and Ara-C treatment and plated in fresh medium. Growth and viability of the cells were measured over time by trypan blue exclusion staining. Data represent the mean ±SD from 3 independent experiments

A. Mean + SD growth and viability of persisting MOLM13 over time starting 20 days post Daunorubicin and Ara-C treatment as measured by trypan blue exclusion staining. Data represent the mean +SD from 3 independent experiments
B. Persisting MOLM13 cells were collected on day 6 after Daunorubicin (40nM) and Ara-C (200nM) treatment and plated in fresh medium to recover until day 20. On day 20 cells were retreated with increasing concentrations of Daunorubicin for 72 hours and growth and viability were measured using Alamar Blue staining. Data represent mean ± SD growth and viability from a representative experiment (n=2).
C. Cell cycle analysis as measured by PI staining and flow cytometry in persisting MOLM13 cells collected on day 6 post Daunorubicin and Ara-C treatment. Data represents mean + SD from a representative experiment (n=2).
D. Wild type and persisting MOLM13 cells were labelled with 5-ethynyl-2′-deoxyuridine (EdU). EdU uptake was measured by flow cytometry 2 and 72 hours post treatment. Data represents mean ± SD from a representative experiment (n=2).
E. MOLM13 control and DTP cells were labeled with CellTrace Violet stain. Staining intensity and dilution over time was measured at day 1 and 5 post-staining using flow cytometry

Figure 2: Lipid composition of leukemic DTP cells

A. MOLM13 cells were treated with the combination of Daunorubicin (40) and Ara-C (200nM respectively) to achieve an IC_{90}. Residual viable cells were collected on day 6 after Daunorubicin and Ara-C treatment for lipidomic analysis. Difference in proportion of phosphatidylcholine (PC) species between DTP and control samples.

Species above the x-axis are enriched in DTP samples, and species below are enriched in untreated samples.

B. Difference in proportion of Triglycerides (TG) species between DTP and control samples. Species above the x-axis are enriched in DTP samples, and species below are enriched in untreated samples.

C. Difference in proportion of Phosphatidylethanolamine (PE) species between DTP and control samples. Species above the x-axis are enriched in DTP samples, and species below are enriched in untreated samples.

D. Heatmap showing abundance of sphingomyelin (SM) species in MOLM13, MV4-11, THP-1 and NB4 cells in the DTP phase (day 6 post-chemotherapy) and in the recovery phase (day +21 post-chemotherapy). Relative fold change levels are indicated on the colour scale, with numbers indicating the log2 fold change normalized to untreated cells.

E. MOLM13 DTP cells were collected on day 6 after Daunorubicin and Ara-C treatment and incubated with BODIPY-FL-C_{16}. BODIPY-FL-C_{16} MFI values measured by flow cytometry. Data represents the mean $\pm$ SD from 3 independent experiments.

Figure 3: Leukemic DTP cells exhibit decreased cell membrane fluidity

A. MOLM13, NB4, OCI-AML2, MV4-11, THP-1 and OCI-AML3 were treated with Daunorubicin + AraC to achieve an IC^{90}. Residual viable cells were collected on day 6 post treatment and stained using the fluorescent PDA probe to assess membrane fluidity. DTP recovery represents DTP cells collected on day 6 post treatment, plated in fresh medium to recover until day 20. The emission fluorescence was quantified using a plate reader in triplicates. Data represents the mean $\pm$ SD of 3 independent experiments. **P < .01; ****P < .0001by student t-test.

B. Schematic illustration showing a patient derived xenograft model. Primary AML cells were injected into the right femurs of sub-lethally irradiated NSG mice. Eight weeks after cell injection, mice were treated with 60 mg/kg/day Ara-C or vehicle for 5 days. DTP cells were collected on day 8 post Ara-C treatment.

C. Primary AML cells were engrafted into NSG mice and treated with Ara-C as in 3b. The percent of AML cells ($CD45^+CD33^+$) engrafted into the mouse femur was measured by flow cytometry. ****P < .0001 by student t-test.

D. Pooled human $CD45^+$ patient-derived DTP cells were collected from mice on day 8 post Ara-C-treatment. Cells were stained using the fluorescent PDA probe to assess membrane fluidity. The emission fluorescence was quantified using a plate reader in triplicates. Data represents mean ± SD. ****P < .0001 by student t-test.

E. Membrane fluidity of blasts cells in paired patient bone marrow samples collected on day 0 and day +5 post-chemotherapy. Cells were stained using the fluorescent PDA probe and membrane fluidity was assessed using flow cytometry and analysis of $CD45^{dim}CD34^+CD117^+$ cell MFI.

Figure 4: Non-pharmacologic models that transiently increase membrane rigidity confer chemoresistance in AML

A. MOLM13 cells were cultured at 31°C for 24 hours prior to analysis, 37°C or 31°C for 24 hours and then transferred back to 37°C (31°C→37°C). Growth and viability of the cells were measured by trypan blue exclusion staining. Data represents mean ± SD of 3 independent experiments.

B. MOLM13 cells from 4A were retreated with increasing concentrations of Daunorubicin and Ara-C for 72 hours and growth and viability were measured using Sulforhodamine B (SRB) assay. Data represents mean ± SD growth from a representative experiment (n=2).

C. MOLM13 cells cultured at 31°C, 37°C or 31°C→37°C were stained using the fluorescent PDA probe to assess membrane fluidity. Emission fluorescence was quantified using a plate reader in triplicates. Data represents the mean ± SD of 3 independent experiments. ****P < .0001 by student t-test.

D. MOLM13 cells treated with cholesterol (60 ug/ml) were stained using the fluorescent PDA probe to assess membrane fluidity. Data represents the mean ± SD of 3 independent experiments. ****P < .0001 by student t-test.

E. Control and cholesterol-treated MOLM13 cells incubated with Daunorubicin at increasing concentrations. Daunorubicin uptake was assessed by flow cytometry.

Data represents the mean ± SD of 3 independent experiments. ****P < .0001 by 2-way ANOVA test.

Figure 5: Increasing cell membrane rigidity sensitizes AML cells to T-cell mediated cytotoxicity

A. MOLM13 and OCI-AML2 cells cultured at 37^0C or 31^0C (24 hours) were incubated with double negative T-cells (DNTs) for 2 hours. Percent specific killing of AML cells by DNTs was determined by Annexin V staining and flow cytometry. Data represents mean ± SD from a representative experiment (n=3). **P < .01 by student t-test.
B. MOLM13 cells engrafted and collected from mice post Ara-C+/- DNT cell injection. Percent engraftment was determined by flow cytometry gating on live human $CD3^-$ $CD45^+$ cells. Data represent mean ± SD (n=7-10). **P < .001 by student t-test.
C. Patient sample (AML 166315) engrafted and collected from mice at day +8 post Ara-C treatment. Pooled human $CD45^+$ cells were incubated with DNT cells for 2 hours. Percent specific killing of AML cells by DNTs was determined by AnnexinV staining in flow cytometry. Data represents mean ± SD (n=3). ***P < .01 by student t-test.
D. CD34+ blast cells were separated from paired bone marrow samples (patient AML#3) collected on day 0 and day +5 post chemotherapy. Cells were incubated with DNT cells for 2 hours. Percent specific killing of CD34+CD117+ blast cells by DNTs was determined by AnnexinV staining in flow cytometry. Data represents mean + SD of (n=3). *P < .05 by student t-test.

Figure 1

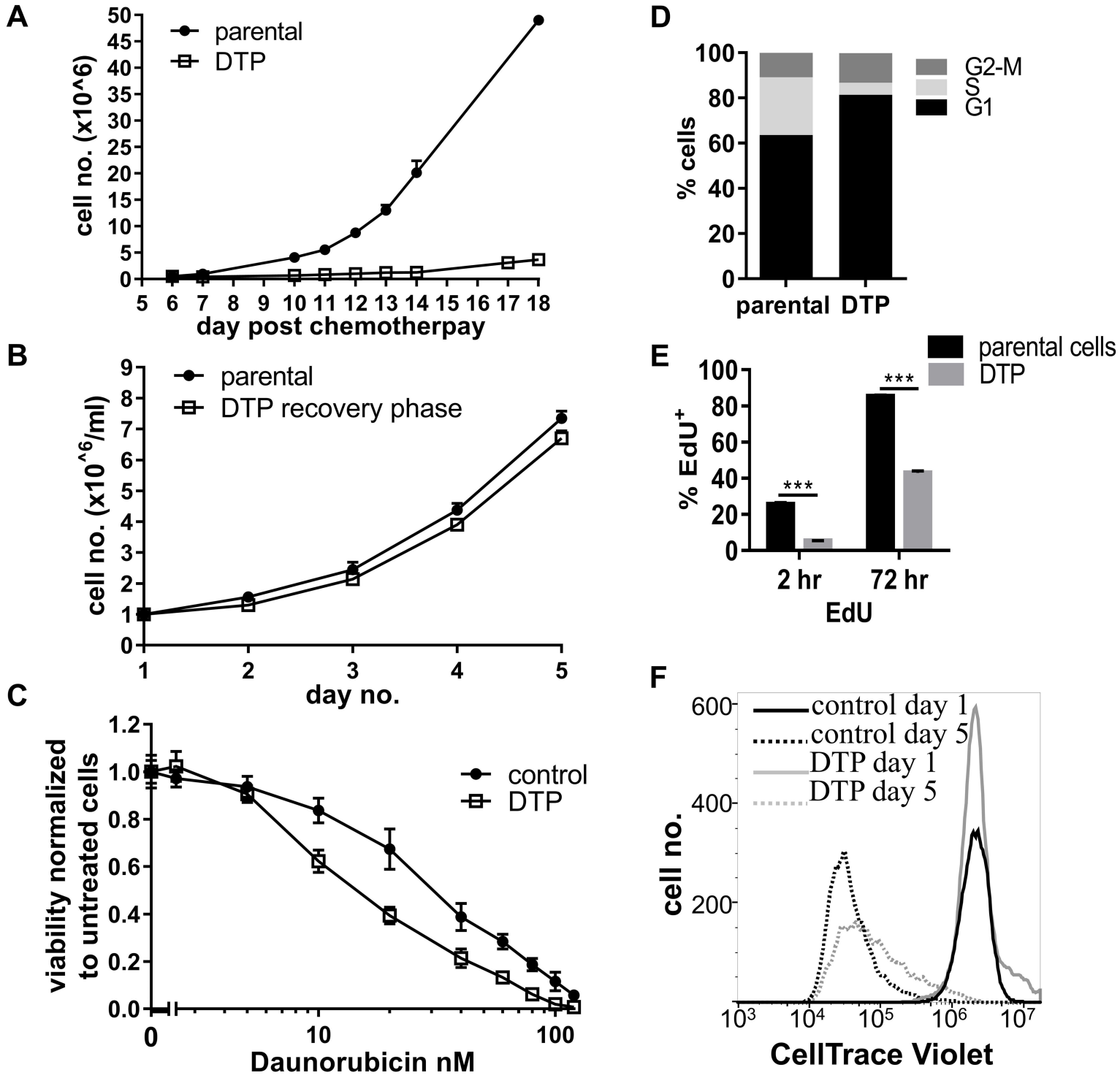
A
parental
DTP
cell no. (x10^6)
day post chemotherpay
B
parental
DTP recovery phase
cell no. (x10^6/ml)
day no.
C
control
DTP
viability normalized to untreated cells
Daunorubicin nM
D
G2-M
S
G1
% cells
parental
DTP
E
parental cells
DTP
% EdU+
***
***
2 hr
72 hr
EdU
F
control day 1
control day 5
DTP day 1
DTP day 5
cell no.
CellTrace Violet

Figure 2

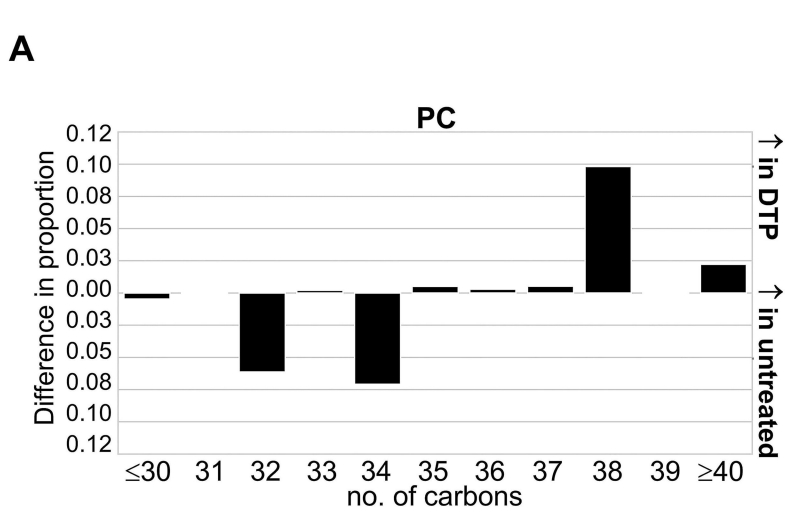
A
PC
Difference in proportion
0.12
0.10
0.08
0.05
0.03
0.00
0.03
0.05
0.08
0.10
0.12
↑ in DTP
↑ in untreated
≤30 31 32 33 34 35 36 37 38 39 ≥40
no. of carbons

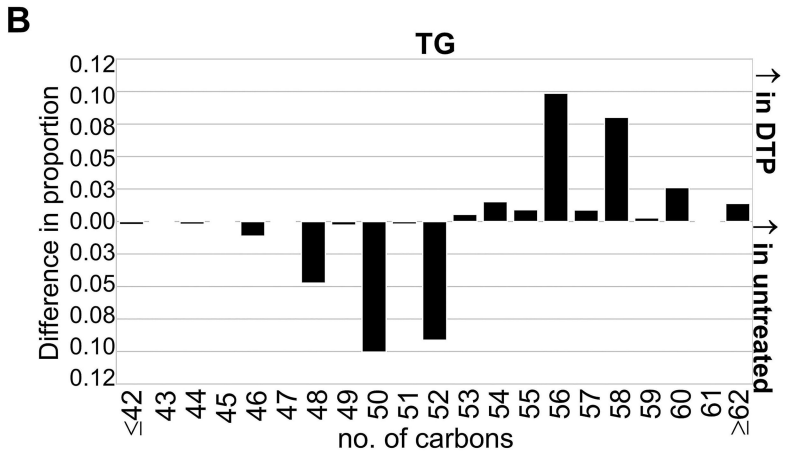
B
TG
Difference in proportion
0.12
0.10
0.08
0.05
0.03
0.00
0.03
0.05
0.08
0.10
0.12
↑ in DTP
↑ in untreated
≤42 43 44 45 46 47 48 49 50 51 52 53 54 55 56 57 58 59 60 61 ≥62
no. of carbons

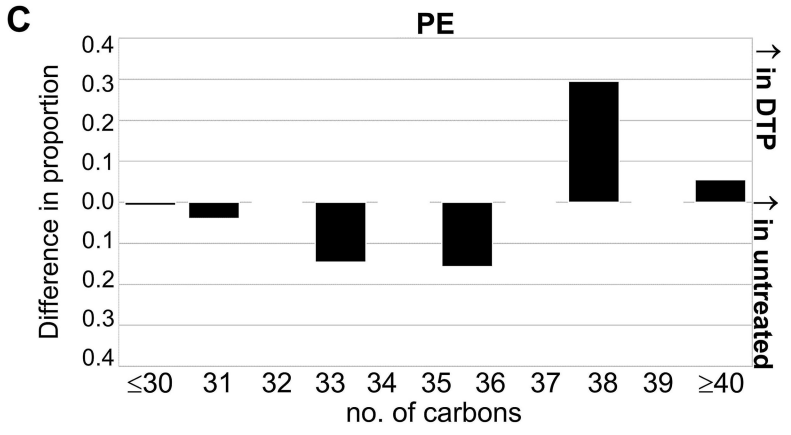
C
PE
Difference in proportion
0.4
0.3
0.2
0.1
0.0
0.1
0.2
0.3
0.4
↑ in DTP
↑ in untreated
≤30 31 32 33 34 35 36 37 38 39 ≥40
no. of carbons

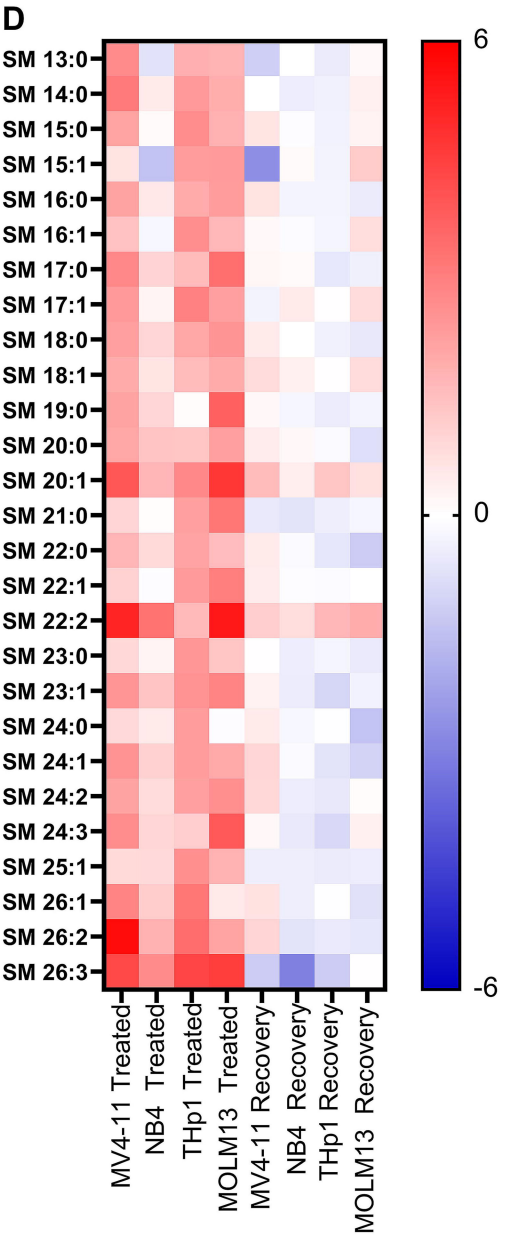
D
SM 13:0
SM 14:0
SM 15:0
SM 15:1
SM 16:0
SM 16:1
SM 17:0
SM 17:1
SM 18:0
SM 18:1
SM 19:0
SM 20:0
SM 20:1
SM 21:0
SM 22:0
SM 22:1
SM 22:2
SM 23:0
SM 23:1
SM 24:0
SM 24:1
SM 24:2
SM 24:3
SM 25:1
SM 26:1
SM 26:2
SM 26:3
MV4-11 Treated
NB4 Treated
THp1 Treated
MOLM13 Treated
MV4-11 Recovery
NB4 Recovery
THp1 Recovery
MOLM13 Recovery
6
0
-6

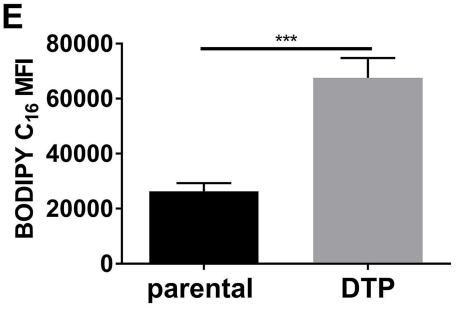
E
***
BODIPY C16 MFI
80000
60000
40000
20000
0
parental
DTP

Figure 3

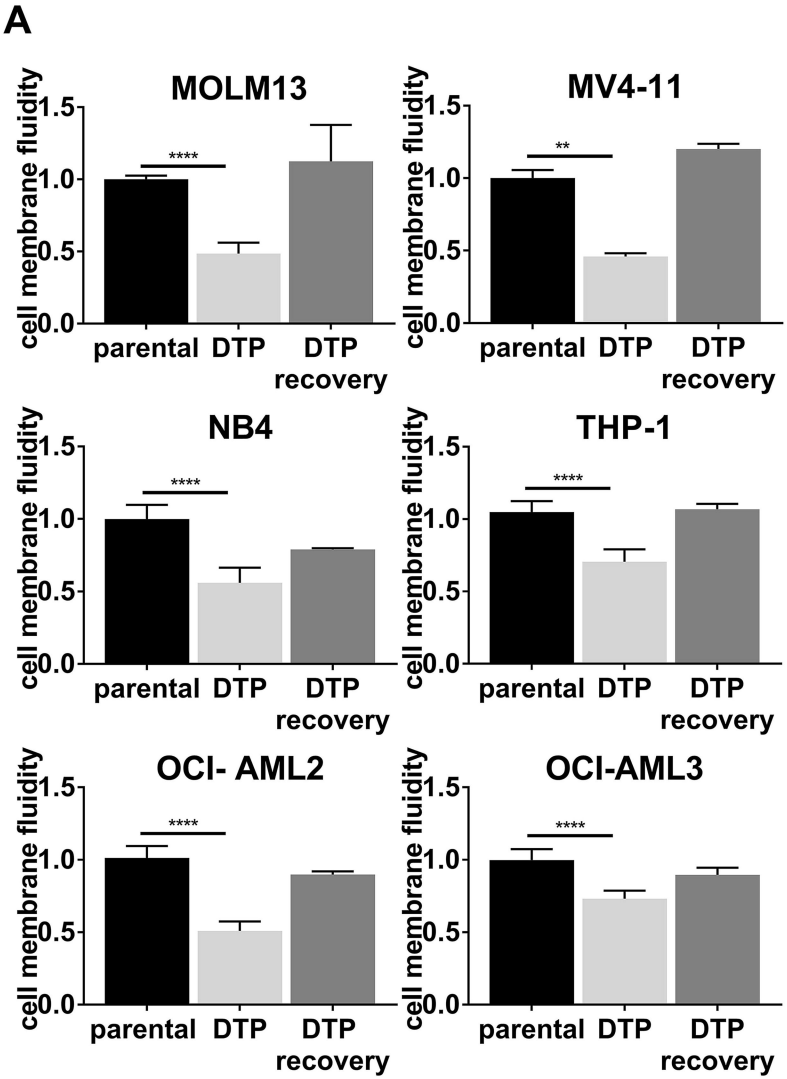
A
MOLM13
MV4-11
NB4
THP-1
OCI- AML2
OCI-AML3
cell membrane fluidity
1.5
1.0
0.5
0.0
****
**
parental
DTP
DTP recovery

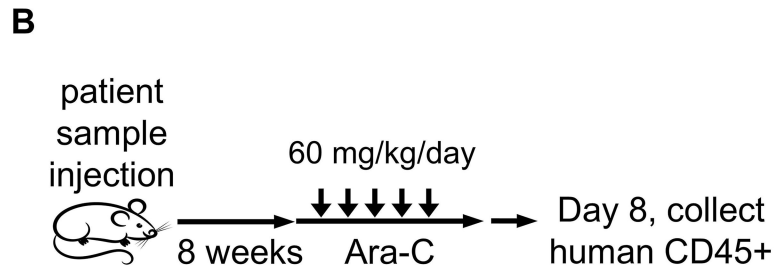
B
patient sample injection
60 mg/kg/day
8 weeks
Ara-C
Day 8, collect human CD45+

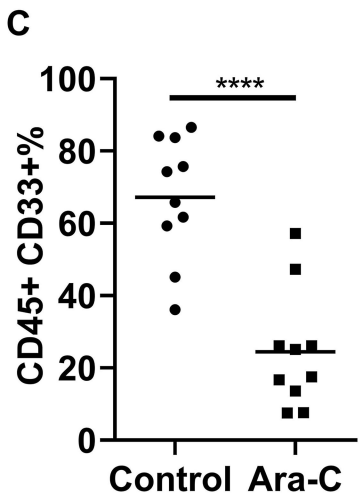
C
CD45+ CD33+%
100
80
60
40
20
0
****
Control
Ara-C

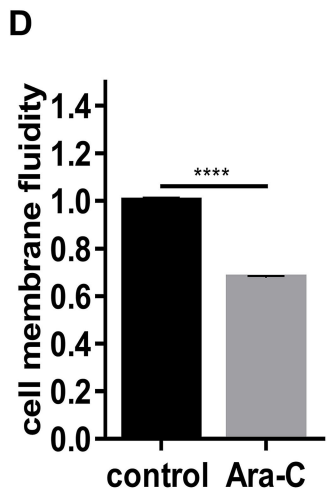
D
cell membrane fluidity
1.4
1.2
1.0
0.8
0.6
0.4
0.2
0.0
****
control
Ara-C

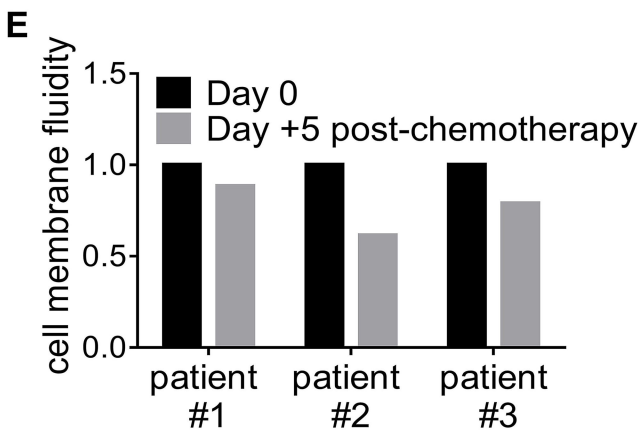
E
cell membrane fluidity
1.5
1.0
0.5
0.0
Day 0
Day +5 post-chemotherapy
patient #1
patient #2
patient #3

Figure 4

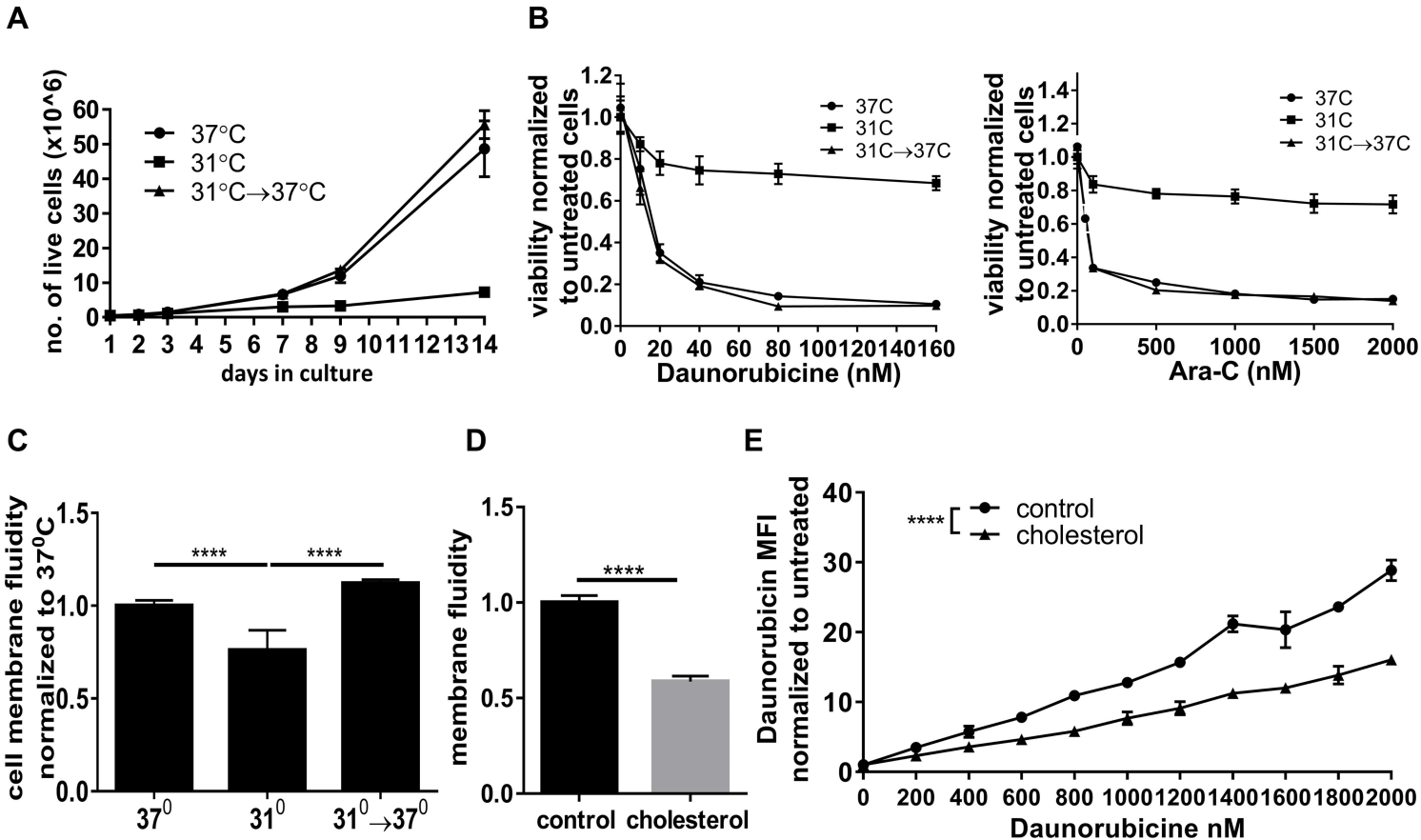
A
no. of live cells (x10^6)
37°C
31°C
31°C→37°C
days in culture
B
viability normalized to untreated cells
37C
31C
31C→37C
Daunorubicine (nM)
Ara-C (nM)
C
cell membrane fluidity normalized to 37°C
****
37⁰
31⁰
31⁰→37⁰
D
membrane fluidity
control
cholesterol
E
Daunorubicin MFI normalized to untreated
control
cholesterol
Daunorubicine nM

Figure 5

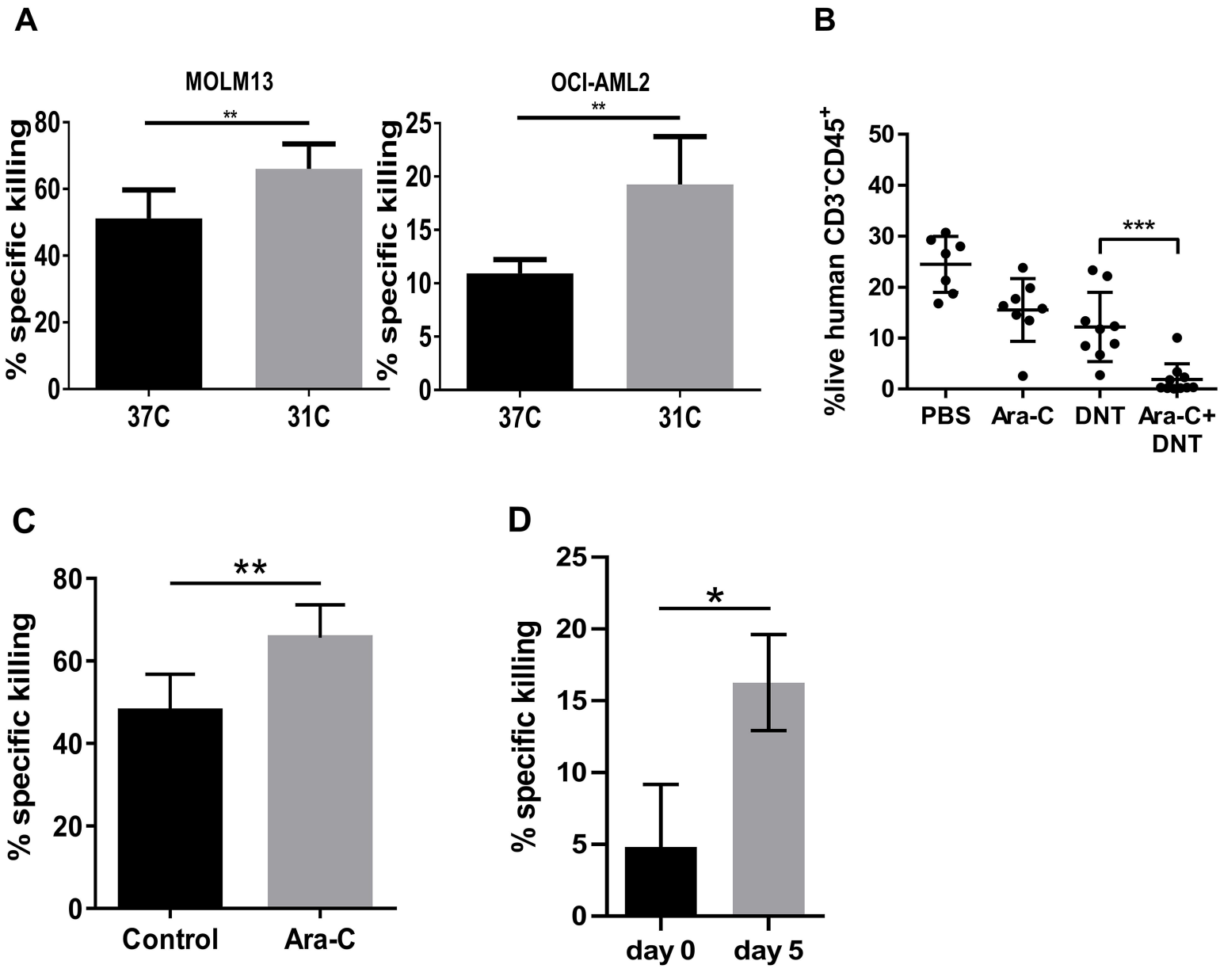
A
MOLM13
OCI-AML2
% specific killing
37C
31C
**
B
%live human CD3-CD45+
PBS
Ara-C
DNT
Ara-C+ DNT
***
C
Control
Ara-C
D
day 0
day 5
*

Supplementary Methods

Cell culture and reagents

MV4-11 and OCI-AML2 cells were cultured in Iscove's modified Dulbecco's medium (IMDM). MOLM13, THP1 and NB4 cells were cultured in RPMI. OCI-AML3 cells were cultured in alpha-MEM medium. All media were supplemented with 10% fetal bovine serum and appropriate antibiotics. All cell lines were maintained in humidified incubators at 37 °C supplemented with 5% CO2. To enrich the plasma membrane of cell lines with cholesterol, cells were incubated overnight with 60 ug/ml water-soluble cholesterol (Sigma-Aldrich, C4951).

Animals

Immunodeficient NOD.Cg-Prkdc^{scid} Il2rg^{tm1Wjl}/SzJ (NSG) mice were obtained from the University Health Network. For the in vivo experiments, the mice were grouped prior to treatment. The grouping and treatment of the mice were performed by an individual who was not involved in the analysis of the data from the experiment. Mice were randomly assigned to each experimental group. During all experiments, the weights of the mice were approximately 18–30 g with no animals losing greater than 10% body weight. All animals were housed in microisolator cages with temperature-controlled conditions under a 12-h light/dark cycle with free access to drinking water, and food. Primary AML cells (1x10^6) were injected into the right femur of pre-conditioned NSG mice (6–10 weeks) that were sub-lethally irradiated (2 Gy) 24h prior to injection. Eight weeks after cell injection, intravenous Ara-C treatment (60 mg/kg/day) was administered for 5 consecutive days. Mice were sacrificed on day 8 post-chemotherapy, and bone marrow samples were collected and processed using standard methods. Leukemic engraftment was determined by flow cytometry gating on the human CD45$^+$CD34$^+$ population. For the DNT killing assay, human CD45$^+$ cells were separated from pooled bone marrows from each treatment group using human magnetic CD45 MicroBeads (Miltenyi Biotec). For the in-vivo DNT killing experiments, MOLM13 cells (1x10^6) were injected into the right femur of pre-conditioned NSG mice sub-lethally irradiated (2 Gy) 24h prior to injection. Three days after cell injection, intravenous Ara-C treatment (40 mg/kg/day) was administered

for 5 consecutive days. 20×10^6 DNTs were then injected i.v. on days 11 and 13 along with rIL2 (Proleukin, 104 IU/mouse). Mice were sacrificed on day14 and engraftment was measured by flow cytometry gating on human $CD3^-CD45^+$ cells. All animal studies were performed in accordance with the University Health Network Animal Use Protocol.

Fatty acid uptake

Fatty acid uptake was assessed using BODIPY-FL-C_{16} (Invitrogen, #D3821). Cells were incubated in media with 1uM BODIPY-C16 for 30 minutes. Fatty acid uptake was measured using flow cytometry measuring the mean fluorescence intensity (MFI) of BODIPY-FL-C_{16}.

Viability

Cell viability following chemotherapy treatment was assessed by Alamar Blue viability kit (Invitrogen) as per the manufacturer's instructions. Viability of cells cultured at 31^0C was assessed using the Sulforhodamine B (SRB) assay following a previously described protocol[51].

Daunorubicin uptake

MOLM13 cells were treated with increasing concentrations of Daunorubicin for 3 hours. Daunorubicin uptake was assessed via the PE channel in flow cytometry.

Flow Cytometry

Flow cytometry analysis was performed on Cytoflex (Beckman Coulter Life Sciences) or LSR Fortessa (BD Biosciences). Data was analyzed post-acquisition with FlowJO Software Version 10.1. Patient samples were stained with anti-CD117 (Biolegend, #313230), anti-CD34 (BD, #560710), anti-CD45 (BD, #564585) antibodies and 7-AAD.

Cell cycle and proliferation analysis

Cells were incubated with EdU (10 uM) for 2 or 72 hours. Cell cycle was assessed using EdU Staining Proliferation Kit (Abcam, #219801) and DAPI, as per the manufacturer's instructions, and analyzed by flow cytometry. For the dye dilution assay, cells were stained

with CellTrace Violet (ThermoFisher, # C34557) according to manufacturer protocol. Dye dilution was determined through flow cytometry on days 1 and 5.

Lipidomics

Lipids were extracted from frozen cell pellets using a methyl tert-butyl ether (MTBE)-based extraction method[52,53]. Dried lipid extracts were reconstituted and analyzed using a Horizon Vanquish UHPLC system coupled to an Orbitrap IQ-X Tribrid Mass Spectrometer (Thermo Fisher Scientific). Raw spectral data were processed and analyzed using MS-DIAL (version 4.9.221218) and the MS-DIAL LipidBlast spectral library (version 68)[54]. To detect drug-/temperature-dependent changes in FA carbon chain lengths among lipids of the same lipid class, distributions of LC-MS signal (area), aggregated by FA carbon chain length and lipid class were compared. First, areas were summed for lipids of the same FA carbon chain length and class. These areas were then normalized to proportion values, which represent proportional contributions by lipids of a particular FA carbon chain length to the total area detected for a lipid class. To do so, each area was divided by the sum of all area values within its respective lipid class. To produce difference plots, difference values were calculated between mean proportion values of lipids with the same FA carbon chain length and class.

DNT killing assay

DNT expansion was performed as previously described[55]. Briefly, healthy donor–derived PBMCs depleted from $CD4^+$ and $CD8^+$ cells were cultured on anti-CD3 antibody-coated plates (OKT3; BioLegend) for 3 days in AIM-V (Thermo Fisher Scientific) with 250 IU/mL of interleukin-2 (IL-2) (Proleukin; Novartis Pharmaceuticals); soluble anti-CD3 antibody, IL-2 and fresh AIM-V were added to the cultures every 2 to 4 days. DNTs cells purity was evaluated by staining cells with fluorochrome-conjugated anti-human CD3, -CD4, -CD8, and -CD56 antibodies followed by flow cytometry analysis. For the killing assay, DNTs were used between days 10 and 20 of culture and co-cultured with target cells for 2 hours at a ratio of 1:2 target cells to DNT cells. Subsequently, cells were stained with anti-human CD3 (HIT3a), CD33 (WM53), CD45 (HI30), and CD34 (561) antibodies and Annexin V

(all from BioLegend) and analyzed by using flow cytometry. Specific killing was calculated by $\frac{\%AnnexinV^{+}_{with\ DNT} - \%AnnexinV^{+}_{without\ DNT}}{100 - \%AnnexinV^{+}_{without\ DNT}}$ x 100, as previously described[56].

Statistical analysis

Statistical tests included unpaired Student's t-test or 2-way ANOVA. Statistical significance was established at $p < 0.05$. Comparable variability between groups was observed in both animal and in vitro studies. Sample sizes were determined based on experimental feasibility and previous experiences managing replicates.

Table S1. Clinical data of primary AML samples

Patient no.	Age	Gender	Diagnosis	Cytogenetics	Molecular
1401	59	M	AML	46,XY	NPM1 undetectable, FLT3-ITD undetectable
0856	52	M	AML	complex	NPM1 undetectable, FLT3-ITD undetectable
1211	57	M	AML post MDS	unsuccessful	NPM1 undetectable, FLT3-ITD undetectable
166315	72	F	AML	47,XX,+8[17]	NPM1 undetectable, FLT3-ITD undetectable

Supplementary Figures

Supplemental Figure 1

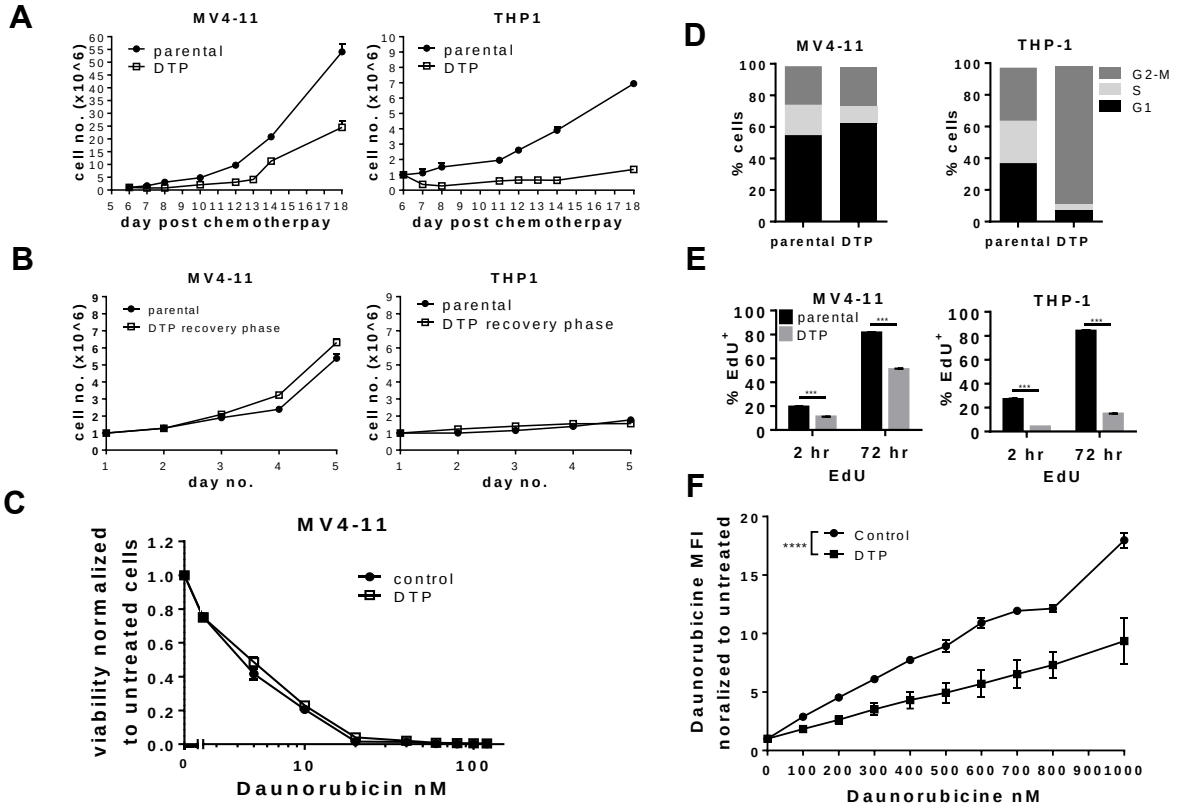

Supplemental Figure 1. AML DTP cells in-vitro model; A. MV4-11 and THP1 drug tolerant persistent (DTP) cells were treated with the combination of Daunorubicin (20 and 90 nM, respectively) and Ara-C (70, and 900 nM respectively) to achieve an IC90. Residual viable cells were collected on day 6 after Daunorubicin and Ara-C treatment and plated in fresh medium. Growth and viability of the cells were measured over time by trypan blue exclusion staining. Data represent the mean +SD from 3 independent experiments. B. Mean + SD growth and viability of persisting MV4-11 and THP1 over time starting 20 days post Daunorubicin and Ara-C treatment as measured by trypan blue exclusion staining. Data represent the mean +SD from 3 independent experiments. C. Persisting MV4-11 cells were collected on day 6 after Daunorubicin (20nM) and Ara- C (70nM) treatment and plated in fresh medium to recover until day 20. On day 20 cells were retreated with increasing concentrations of Daunorubicin for 72 hours and growth and viability were measured using Alamar Blue staining. Data represent mean+SD growth and viability from a representative experiment (n=2). D. Cell cycle analysis as measured by PI staining and flow cytometry in persisting MV4-11, and THP1 cells collected on day 6 post Daunorubicin and Ara-C treatment. Data represents mean + SD from a representative experiment (n=2). E. Wild type and persisting MV411, and THP1 cells were labelled with EdU. EdU uptake was measured by flow cytometry 2 and 72 hours post treatment. Data represents mean + SD from a representative experiment (n=2). F. Control and DTP MOLM13 cells incubated with Daunorubicin at increasing concentrations. Daunorubicin uptake was assessed by flow cytometry. Data represents the mean + SD of 3 independent experiments. ****P < .0001 by 2-way ANOVA test.

Supplemental Figure 2

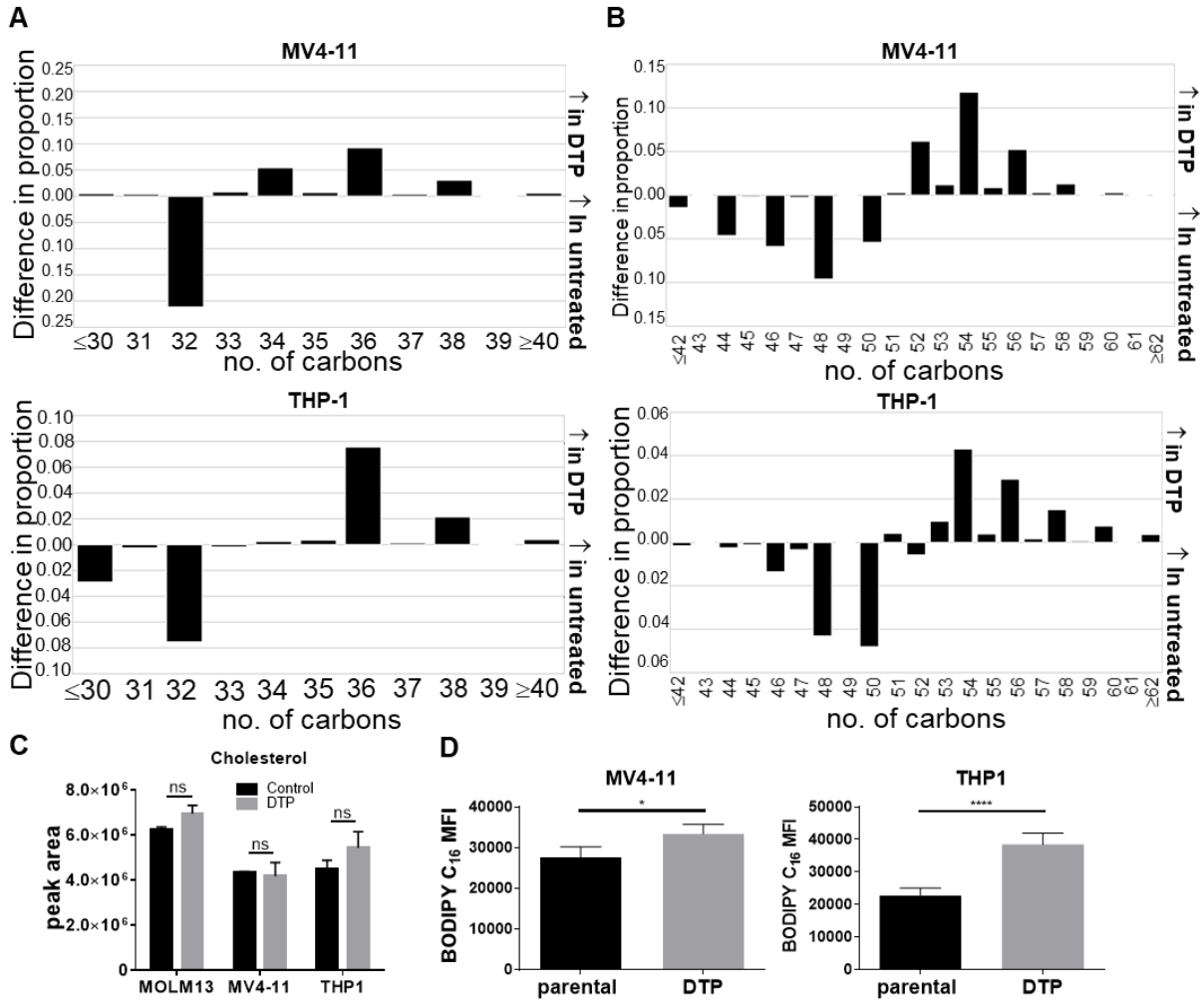

Supplemental Figure 2. Lipid composition in DTP cells; **A.** Difference in proportion of PC (phosphatidylcholine) species between DTP and control samples in MV4-11 and THP1 cell lines. Species above the x-axis are enriched in control samples, and species below are enriched in DTP samples. **B.** Difference in proportion of TG (Triglycerides) species between DTP and control samples in MV4-11 and THP1 cell lines. **C.** Cholesterol levels of MOLM13, MV4-11 and THP-1 DTP cells collected on day 6 after Daunorubicin and Ara-C treatment. Data represents the mean ± SD (n=3). **D.** MV41-11 and THP1 DTP cells were collected on day 6 after Daunorubicin and Ara-C treatment and incubated with BODIPY-FL-C16. BODIPY-FL-C16 MFI values measured by flow cytometry. Data represents the mean ± SD from 3 independent experiments.

Supplemental Figure 3

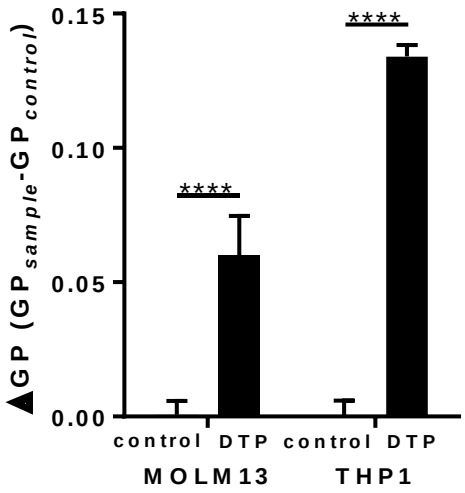

Supplemental Figure 3. Leukemic DTP cells exhibit decreased cell membrane fluidity. Quantiative analysis of di-4-ANEPPDHQ generalized polarization (GP) in MOLM13 and THP1 cells as measured by flow cytometry. Data represents the mean+SD of 3 independent experiments. **** $P < .0001$ by student t-test.